Climate suitability of East Asian mangroves for nature-based solutions is limited by climate extremes

Ran Chen[1,2], Jin-Soo Kim[1,2,3*], Jung-Eun Chu[1,4*], Hyo-Jeong Kim[1,2], Bora Lee[5], Sujong Jeong[6], Gabriela Schaepman-Strub[7]

[1]School of Energy and Environment, City University of Hong Kong, Hong Kong, People's Republic of China
[2]Center for Ocean Research in Hong Kong and Macao (CORE), The Hong Kong University of Science and Technology, Hong Kong, People's Republic of China
[3]Department of Civil and Environmental Engineering, Korea Advanced Institute of Science and Technology, Daejeon, Republic of Korea
[4]School of Earth and Environmental Sciences, Seoul National University, Seoul, Republic of Korea
[5]Warm-Temperate and Subtropical Forest Research Center, National Institute of Forest Science, Jeju, Republic of Korea
[6]Department of Environmental Planning, Seoul National University, Seoul, Republic of Korea
[7]Department of Evolutionary Biology and Environmental Studies, University of Zurich, Zurich, Switzerland

Correspondence to: Jin-Soo Kim (jinsoo@kaist.ac.kr) and Jung-Eun Chu (jungeunchu@snu.ac.kr)

Abstract. Mangroves represent distinctive coastal ecosystems that offer ecological benefits, notably through their high carbon sequestration rates. However, their resilience to extreme climate events remains uncertain. Here, we investigated the response of mangroves in East Asia to climate variability by employing the remote-sensing derived Normalized Difference Vegetation Index (NDVI) as a proxy for canopy greenness. A bootstrapping-based statistical framework was applied to identify vegetation responses associated with extreme climate events and quantify lagged climatic effects. We found East Asian mangrove NDVI variability was strongly influenced by preceding winter temperature and seasonal solar radiation, with distinct lagged responses on seasonal time scales across latitudinal zones. These findings were extrapolated to future projections by the Earth system modelling to assess future climate suitability for existing mangroves and for areas of potential thermal suitability in East Asia, particularly China, South Korea and Japan. These projections assess climatic suitability only and do not account for intertidal habitat availability, coastal geomorphology, or dispersal constraints. While shifts in wintertime isotherms suggest a northward shift in the thermal range of mangroves under global warming, low solar radiation events associated with aerosol emissions under the high-emission SSP3-7.0 scenario could constrain future climatic suitability for mangroves. This study highlights that both temperature-driven opportunities and solar radiation constraints should be integrated into practical planning for future conservation, restoration, and migration as nature-based climate solutions.

1 Introduction

Mangroves are vital intertidal ecosystems that provide a wide range of ecosystem services, including the provision of food and timber, coastal protection, pollution mitigation, biodiversity conservation and carbon sequestration (Barbier et al., 2011).

As a crucial component of blue carbon ecosystems, mangrove forests—often described as coastal guardians—are one of the most carbon-rich ecosystems, storing on average ~1,000 Mg C ha^{-1}, with 49–98% carbon stored in the soil (Donato et al., 2011). This carbon storage capacity is roughly five times greater than that of terrestrial tropical forests (Donato et al., 2011). Despite their ecological and climatic significance, mangrove areas have experienced a substantial decline of 30–50% over the past fifty years, primarily due to anthropogenic pressures such as aquaculture expansion, overharvesting and land encroachment (Duke et al., 2007). Such widespread loss has led to a reduction of ecosystem services, notably weakening coastal protection against storm surges and tsunamis (Gultom et al., 2021; Xu et al., 2024). In response to these losses, mangrove protection and restoration have been adopted by many countries as an important nature-based solution (NbS) for climate change mitigation (Macreadie et al., 2021). For example, Indonesia has set an ambitious target to rehabilitate 600,000 ha of mangroves by 2024 (Sasmito et al., 2023). China has increased its mangrove coverage by 17% from 2001 to 2015 through concerted restoration efforts (Jia et al., 2018). Although these restoration initiatives have slowed the rate of mangrove loss in recent years, future changes in mangrove habitat suitability are expected to be more complex, driven by diverse factors such as land use change, sea level rise, and extreme weather events (Goldberg et al., 2020; Friess et al., 2022b). Among these, extreme weather events have contributed to approximately 11% of total mangrove losses, highlighting their importance (Goldberg et al., 2020).

Globally, mangroves predominantly inhabit tropical and subtropical coastal zones between 30°S and 30°N latitude (Jia et al., 2023). In East Asia, they are mainly distributed along the southeastern coast of China and the southern islands of Japan (Kainuma et al., 2013). While this region accounts for only 0.1–0.2% of global mangrove coverage (Jia et al., 2023; Kainuma et al., 2013), its carbon sequestration potential and restoration capacity are considerable. It was reported that mangroves in China store approximately 355±82 Mg C ha^{-1}, while in Japan, coastal ecosystems including mangroves are estimated to account for about 4% of national CO_2 uptake by 2030, with an upper-limit estimate of 12% (Liu et al., 2014; Kuwae et al., 2023). In South Korea, several coastal regions already host semi-mangrove species (e.g. *Hibiscus hamabo* and *Paliurus ramosissimus* in Jeju Island), and ongoing studies are exploring the potential introduction of true mangrove species to the Korean peninsula to cope with climate crisis (Lee and Baral, 2023; Lee et al., 2023). However, it remains unclear whether future climate change will create favourable conditions for mangrove expansion, not only within their current habitats but also in newly suitable areas resulting from potential northward range shifts under global warming. A better understanding of how future climate conditions influence mangrove growth and habitat suitability could therefore help inform long-term management and Nationally Determined Contributions (NDCs) planning in East Asian countries.

Temperature, solar radiation and precipitation are widely recognized as three fundamental drivers of vegetation dynamics, although their magnitude, seasonal variability, and lagged responses can vary substantially across regions (Ding et al., 2020; Nemani et al., 2003). In many terrestrial ecosystems, precipitation is commonly used as a proxy for water availability. However, compared with most terrestrial ecosystems, mangroves typically occur in intertidal environments where water is physically abundant but largely saline. Under such conditions, the availability of usable water for mangroves is regulated by complex hydrological and physiological processes rather than precipitation alone. Mangroves therefore rely on specialized

water acquisition mechanisms, including root uptake from a saline environment and foliar water absorption in some species (Reef and Lovelock, 2015), which means that precipitation alone may not adequately represent water availability for mangroves. Therefore, this study focuses on temperature and solar radiation as the primary climatic variables influencing mangrove vegetation dynamics.

Despite the recognized importance of these climatic drivers, long-term quantitative assessments of their influence on mangrove growth remain limited. Most existing research relied on experimental, field, or remote sensing observations over relatively short time scales (Chen et al., 2017; Luo and Chui, 2020; Zheng et al., 2016). Therefore, this study quantifies the impacts of temperature and solar radiation on mangrove canopy greenness and further evaluates how future climate change may alter climatic conditions relevant to mangrove growth in East Asia. These findings provide a scientific basis for evidence-based conservation and restoration strategies targeting mangrove ecosystems.

2 Methods

2.1 Study area

The study focuses on mangroves distributed along the South China Sea. Mangrove distribution data were obtained from the Global Mangrove Watch (Bunting et al., 2022), which provides long-term observations that cover the study period. Based on climatic conditions and dominant species composition across the natural latitudinal range of mangroves in this region (Zhao et al., 2024) (Table S1), mangrove habitats were further classified into three distinct zones (northern, middle, and southern) for comparison. These zones exhibit clear thermal gradients, with mean winter temperatures of approximately 14.5 °C, 16.6 °C, and 19.1 °C in the northern, middle, and southern zones, respectively.

2.2 Datasets

The study period spans from 2001 to 2022. Mangrove vegetation dynamics were assessed based on Normalized Difference Vegetation Index (NDVI), a widely used index for quantifying vegetation health and density using remote sensing spectrum (Tran et al., 2022). Based on the optical properties of vegetation photosynthesis, NDVI is calculated as follows:

$$NDVI = (\rho NIR - \rho RED)/(\rho NIR + \rho RED), \quad (1)$$

where ρNIR is the surface reflectance in the near infrared band, and ρRED is the surface reflectance in the red band. In this study, NDVI data were obtained directly from remote sensing dataset MODIS Vegetation Indices (MOD13Q1) Version 6.1 from 2001 to 2022 (Didan, 2021), with a composite of every 16 days for temporal resolution and a spatial resolution of 250 m. Climate data, including mean temperature and surface solar radiation downwards, were obtained from European Centre for Medium-Range Weather Forecasts Reanalysis v5 (ERA5) for climatic analysis (Hersbach et al., 2023), with the time range from 2001 to 2022 and the spatial resolution at 0.25°×0.25°. The reanalysis data provide spatiotemporally continuous datasets compared with observational data, which is especially helpful for the analysis on mangroves as they are located in

the intertidal areas where direct observations are often sparse. Total bright sunshine, defined as the sum of the time for which the direct sunshine irradiance exceeds 120 W/m^2, was obtained from Hong Kong Observatory. The future projections for climate conditions were investigated using projections from 28 coupled Earth System Models incorporated in the Coupled Model Intercomparison Project Phase 6 (CMIP6). The models are listed in the Table S2. To ensure spatial consistency for observational analysis, ERA5 climate variables were interpolated from 0.25° to match the 250 m spatial resolution of the NDVI dataset. Future climate projections from CMIP6 were analysed at a spatial resolution consistent with the native resolution of the reanalysis data. Here, the coarser resolution of the climate data was considered suitable because the analysis aimed to capture climatic conditions at a regional spatial scale rather than at the individual mangrove pixel level.

2.3 Data pre-processing

NDVI pixels were further extracted for mangroves based on the following rules. First, we selected undisturbed mangrove stands that continuously maintained ≥ 60% canopy coverage during 1996–2020, ensuring that the NDVI values reliably represented mangroves. This period was selected based on the temporal coverage of the mangrove dataset, and to provide a sufficiently long baseline overlapping with the study period. The coverage criterion aligns with protocols from previous related research (Zhang et al., 2024b), with the 60% coverage threshold consistent with the classification scheme of the MODIS Land Cover Type Yearly Global product (MCD12Q1) (Sulla-Menashe and Friedl, 2018). Second, pixels with NDVI ≤0.1 in at least one-third of temporal observations were excluded to minimize abnormal cases (Zuzulova and Vido, 2018). The filtered mangrove NDVI dataset was then used for subsequent analyses. The climate data for the mangrove region were extracted without the coverage threshold rules, considering that the spatial resolution of the climate data was coarser than that of the NDVI dataset. For forest extraction, we selected pixels for evergreen broadleaf forests that remained unchanged from 2001 to 2022 from MCD12Q1. These pixels located within a 2-km buffer around the undisturbed mangroves were then identified and intersected with the NDVI dataset to extract forest NDVI values. The 2-km buffer was used to define the local neighbourhood around undisturbed mangroves. Subsequent data extraction for the forest followed the same procedures as those applied to the mangroves. Both the NDVI data and the climate data were resampled to monthly intervals. The related process was conducted in ArcGIS Pro 3.0 and Python 3.11.6.

2.4 Regression-based sensitivity analysis

The extracted NDVI data and the corresponding climate data were spatially aggregated by averaging within the three zones defined in Sect. 2.1. We applied linear regression to estimate the sensitivity of mangrove NDVI to different climate factors in each zone, with statistical significance assessed using a standard two-tailed Student's *t*-test. The analysis was conducted on monthly detrended anomalies of both NDVI (Y) and climate factors (X) to minimize the influence of long-term trends. The monthly anomalies, calculated as deviations from the corresponding long-term monthly mean for 2001–2022, were detrended using a linear regression approach. To improve the readability and numerical precision of the results, the

sensitivity coefficients were rescaled by factors of 100 for temperature and 1000 for solar radiation, yielding values within a single-digit range (< 10).

2.5 Bootstrapping analysis for extreme cases and lag effect

The basic idea of bootstrapping is to resample the data through randomly picking thousands of times (10,000 iterations in this study) to regenerate an empirical estimate of the entire sampling distribution (Mooney and Duval, 1993). In this research, bootstrapping resampling was applied in both the extreme-case test and time-lagged effect analysis based on the spatially aggregated data within each zone. For the extreme-case test, we examined the relationship between extremely low NDVI anomalies and extremely low values of climate factors, using monthly detrended anomalies. Specifically, the lowest 10% of NDVI anomalies were selected, and the corresponding climate conditions were evaluated against the bootstrapped climate distribution using a one-sided percentile-based test, with the reported *P*–value defined as the empirical one-sided tail probability of the observed mean climate anomaly. Statistical significance was defined as $P < 0.10$, with stronger evidence at $P < 0.05$; these thresholds were applied to all subsequent significance tests in this study. The analysis was conducted at both the annual scale (Fig. 2c, 2e) and the seasonal scale, where boreal seasons (December–January–February, DJF; March–April–May, MAM; June–July–August, JJA; September–October–November, SON) were considered separately (Fig. 2d, 2f; Fig. S2). For the lag-effect test, we assessed the delayed influence of climate factors on mangrove canopy greenness. The analysis was based on boreal seasonal composites of detrended anomalies, with moving windows adjusted to represent different temporal lags. For example, for MAM NDVI, a 0-month lag corresponds to its relationship with MAM climate factors, whereas a 1-month lag corresponds to FMA climate factors. Similar temporal offsets were applied for other seasons and lag periods. In all cases, both NDVI and climate variables were firstly averaged into the three-month seasonal composites. The test was conducted by selecting the high and low NDVI cases (defined as NDVI anomalies exceeding ±1 SD) and evaluating the corresponding climate conditions against the bootstrapped climate distribution using the percentile-based method (Fig. 3). High-NDVI cases were evaluated against the upper tail and low-NDVI cases against the lower tail, with the reported *P*–values representing the corresponding empirical one-sided tail probabilities. To further evaluate the importance of lag effects, we applied the same bootstrap percentile-based test to the difference in climate conditions between high and low NDVI cases, with the reported *P*–values representing the empirical one-sided upper-tail probability of the observed difference (Fig. S3).

2.6 Future projections in the sampled region

We adopted the critical biological temperature threshold of 10 °C in DJF, identified for the mangrove species *Kandelia obovata* in Fujian Province (Wang et al., 2022), as the criterion for delineating the future thermal range of mangroves in East Asia. Two scenarios were selected for comparison: SSP1-2.6, representing a sustainable development pathway consistent with limiting warming to below 2 °C, and SSP3-7.0, representing a high-emission, regional-rivalry pathway with limited climate mitigation (Meinshausen et al., 2020). The baseline 10 °C DJF isotherm for 2001–2022 was derived by combining

CMIP6 historical simulations for 2001–2014 with SSP5-8.5 simulations for 2015–2022. This baseline was compared with the corresponding isotherms projected under SSP1-2.6 and SSP3-7.0 for 2081–2100 (Fig. 4a–b). We identified the season during which solar radiation exerted the strongest influence on mangroves for each zone, based on the results of the time-lagged analysis (Fig. 3d). We then calculated the number of low solar radiation events in that season at the monthly scale. Based on the positive relationship between extreme NDVI and solar radiation, the threshold value for low solar radiation was defined as the mean solar radiation associated with NDVI anomalies below −1 SD during the 2001–2022 reference period. Monthly solar radiation values below this threshold were then identified as low solar radiation events, and their frequency was expressed as the number of events per decade. This analysis was repeated for the historical (1940–2014), SSP1-2.6 (2015–2100) and SSP3-7.0 (2015–2100) periods, respectively (Fig. 4c–e). To address the confidence interval, we derived the event rate from ERA5 (1940–2024) and estimated 2.5th and 97.5th percentiles using bootstrapping resampling. These values were used as the observational estimate for emergent constraint (EC), an approach that derives constraints by correlating model ensemble results with observational estimates (Winkler et al., 2019).

2.7 Future projection in the potential region

To assess the potential northward shifts in the thermal range of mangroves across East Asia (China, South Korea, and Japan), we adopted the 10 °C mean temperature threshold in DJF as the criterion. This thermal range was identified through two steps: (1) selecting current non-mangrove shorelines at a spatial resolution of 0.25°×0.25°, and (2) identifying regions where winter mean temperatures are projected to reach ≥ 10 °C for 2071–2100 under the respective scenario: SSP3-7.0 for Fig. 5 and SSP1-2.6 for Fig. S4. We quantified historical-to-future changes in climatic factors on certain seasonal composites through a multi-model ensemble analysis under historical (1981–2010) and future projections under SSP3-7.0 and SSP1-2.6 (2071–2100) (Fig.5; Fig. S4). These results were compared with the statistically significant thresholds derived from the current northern distribution zone, where the high-temperature threshold was defined as the mean temperature associated with NDVI anomalies above +1 SD, and the low-solar-radiation threshold as the mean solar radiation associated with NDVI anomalies below −1 SD (Fig. 3a, 3d).

3 Results

3.1 Spatial-temporal patterns of mangrove NDVI

Mangroves along the South China Sea were divided into three zones (Fig. 1a), and the seasonal cycle of NDVI reveals clear phenological differences among them (Fig. 1b). This pattern is consistent with previous studies indicating that, despite being evergreen, mangrove forests exhibit notable seasonal and spatial variability (Pastor-Guzman et al., 2018). The northern zone has generally lower values, and the amplitude of NDVI fluctuation decreases progressively from north to south. While both the northern and southern zones exhibit synchronized timing of NDVI maxima and minima—typically with minimum values in winter and maximum values in summer, reflecting the seasonal cycle of temperature—the middle zone demonstrates a

markedly different phenological pattern. Specifically, in the middle zone, NDVI reaches its minimum in March and maximum in October, indicating a shift in the seasonal cycle relative to the other zones. This divergence suggests that, whereas NDVI dynamics in the northern and southern zones are more aligned with temperature seasonality with a potential lag, in the middle zone, NDVI variations are more strongly synchronized with fluctuations in sunshine hours rather than temperature (Fig. S1).

Annual NDVI distribution further reveals strong latitudinal dependencies, with higher and more clustered NDVI values observed at lower latitudes, potentially reflecting more favourable climatic conditions, particularly temperature, for maintaining higher mangrove canopy greenness (Fig. 1c) (Chen et al., 2017). Maximum NDVI values are concentrated at higher values in the middle and southern zones, while the northern zone exhibits lower and more broadly distributed mean and maximum NDVI values.

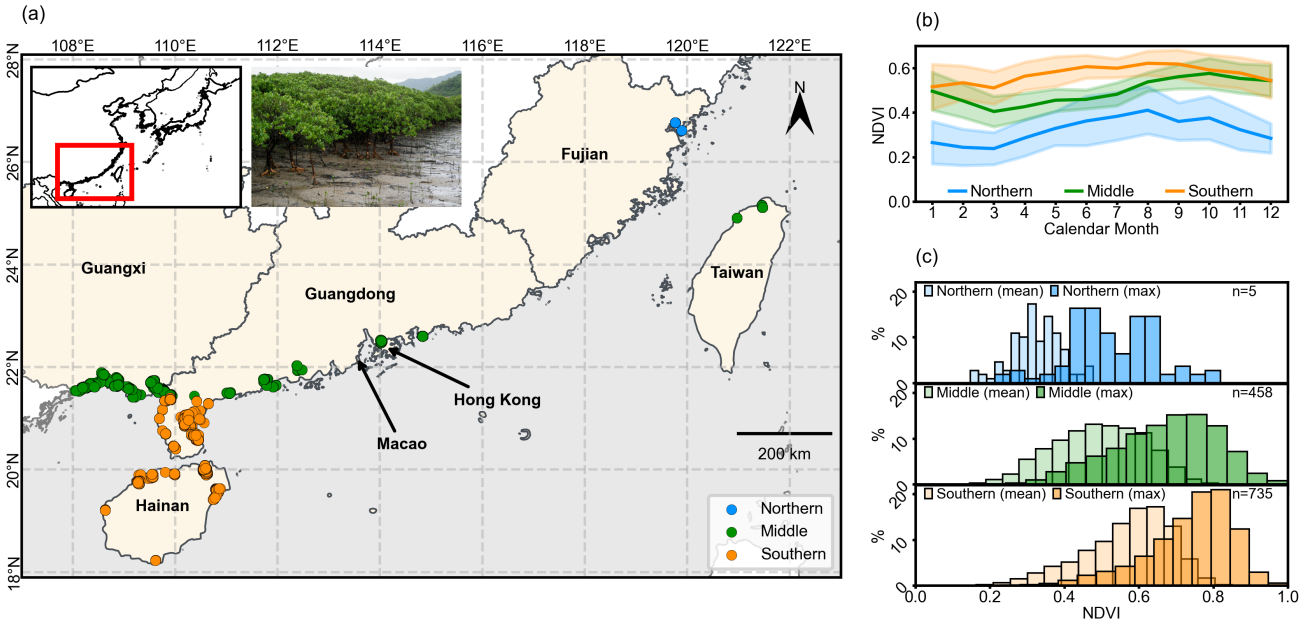


Figure 1. Spatial distribution of sampled mangroves with zone classification and NDVI characteristics. (a) Spatial distribution of sampled mangroves with a pixel resolution of 250 m. Sampling criteria required: (i) undisturbed mangrove stands maintaining ≥60% canopy coverage continuously from 1996 to 2020, and (ii) exclusion of pixels where NDVI ≤0.1 occurred in at least one-third of temporal observations (see Methods). Sampled mangroves were divided into three zones based on species composition, designated as northern, middle, and southern zones. (b) Seasonal cycle of sampled mangrove NDVI from 2001 to 2022. The light-shaded area represents the range of mean ±1 SD. (c) Histogram of yearly maximum and mean NDVI from 2001 to 2022. In the top right corner, *n* represents the number of pixels sampled for each zone.

3.2 Mangrove NDVI responses to temperature and solar radiation forcing

Linear relations between mangrove NDVI in each zone and climatic drivers were quantified to determine the sensitivity of mangrove NDVI to climatic drivers. The sensitivity of mangrove NDVI to temperature does not show consistent patterns

across three zones (Fig. 2a). In contrast, a predominantly positive NDVI response to solar radiation emerges as a notable and consistent pattern in the middle and southern zones (Fig. 2b).

To investigate non-linear response and impact from climate extreme events, we further employed a bootstrapping resampling approach to determine the influence of climate conditions during extreme NDVI events (defined as the lowest 10% of NDVI anomalies). Analysis of the annual NDVI range reveals a marginally significant association with temperature in the southern zone ($P = 0.070$, Fig. 2c) and strong associations with solar radiation in both the southern and the middle zones ($P < 0.01$, Fig. 2e). These results indicate that extremely low NDVI tends to occur under extreme climatic conditions.

Further analysis based on seasonal ranges reveals additional spatial and temporal patterns (Fig. 2d, 2f; Fig. S2). In the middle zone, both temperature and solar radiation exhibit significant relationships with NDVI during MAM ($P = 0.045$, Fig. 2d; $P = 0.006$, Fig. S2d), coinciding with a pronounced NDVI decline during winter-to-spring transition (Fig. 1b). This highlights MAM as a key season for NDVI variability in this region. In the southern zone, significant associations with both temperature and solar radiation are observed during JJA ($P = 0.055$, Fig. S2b; $P = 0.020$, Fig. S2e), consistent with the prevalence of thermophilic stenotopic species in this area (Wu et al., 2018).

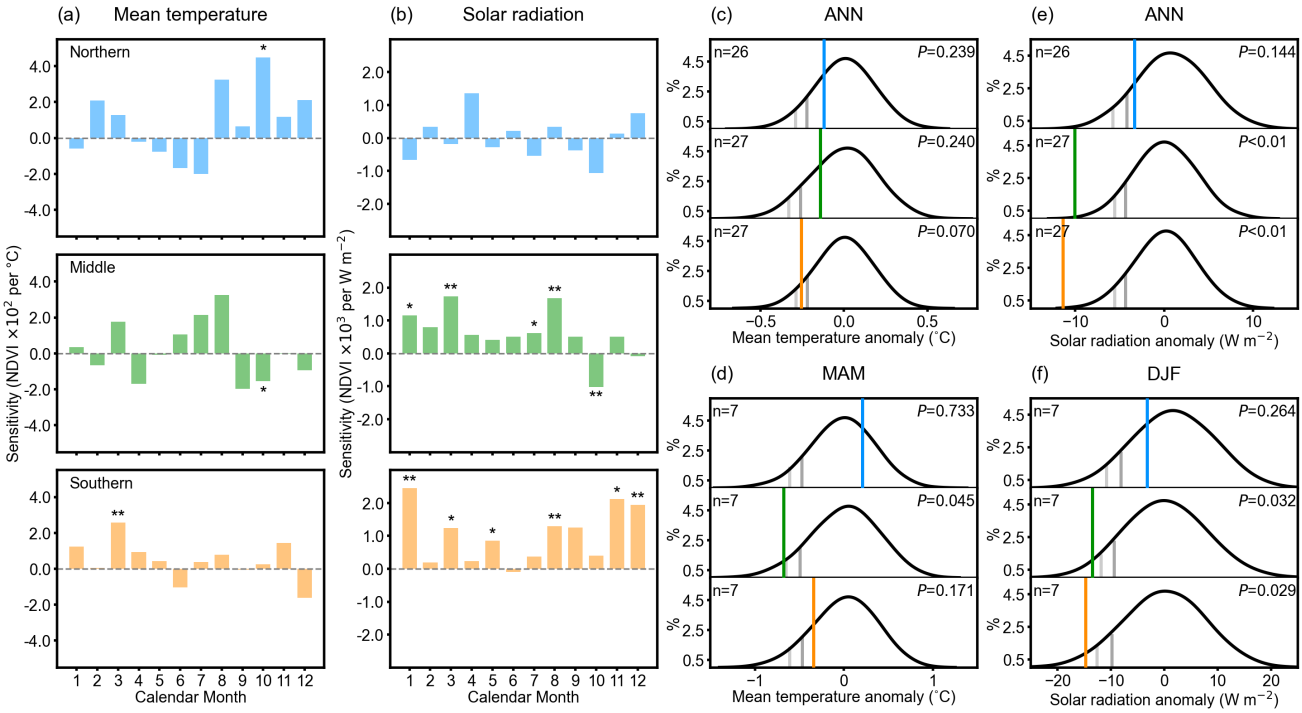


Figure 2. Simultaneous impact of mean temperature and solar radiation on mangrove greenness. Sensitivity of mangrove NDVI to mean temperature (a) and solar radiation (b). Sensitivity is defined as the linear regression slope between monthly NDVI anomalies and climatic anomalies. One asterisk (*) indicates a *P*–value less than 0.1, and two asterisks (**) indicate a *P*–value less than 0.05. Bootstrap distributions for mean temperature and the significance test for extreme low cases are shown for annual (c) and MAM (d), while results for solar radiation are presented for annual (e) and DJF (f). Light grey lines represent $P = 0.05$, and dark grey lines represent $P = 0.1$. In the top left corner, n represents the number of cases selected. In the top right corner, *P* indicates the *P*–value result for the cases and is rounded to three decimal places. Different colours indicate different zones: blue for the northern zone, green for the middle zone and orange for the southern zone.

3.3 Time-lagged effect of climate drivers on seasonal composite NDVI

While extreme NDVI cases are associated with simultaneous climatic anomalies (Fig. 2), we further investigated the potential lagged effect of climatic variables using seasonal composite NDVI and anomalous case detection (defined as NDVI anomalies exceeding ±1 SD). Our results indicate that NDVI during MAM tends to strongly depend on preceding winter temperatures (Fig. 3a, c), providing clear evidence for a legacy effect of winter thermal conditions on subsequent spring mangrove growth. This pattern is particularly evident in the northern zone, where high MAM NDVI cases are significantly associated with temperature anomalies occurring simultaneously and 1–3 months prior (Fig. 3a). In contrast, low MAM NDVI cases in the middle and southern zones also demonstrate lagged temperature effects (Fig. 3c). Furthermore, our analysis highlights the importance of high temperature for mangrove growth during SON, as evidenced by significant short lag (≤1 month) effects (Fig. 3a).

Low solar radiation events during DJF in the low-latitude zone are significantly associated with low NDVI (Fig. 2f), indicating that the influence of radiation in winter is primarily simultaneous. Beyond the winter period, however, the impact of solar radiation on mangroves is primarily evident through lagged responses. For high NDVI cases, elevated solar radiation is significantly associated with JJA in the northern zone at lags of 0 and 2 months and in the middle zone at a lag of 2 months (Fig. 3b), and with SON in the southern zone at a lag of 1 month, highlighting the importance of these transitional seasons. In contrast, low NDVI cases exhibit divergent lagged responses: the northern zone shows a 2–3 month lag to radiation deficits in SON, the middle zone shows a 1-month lag in MAM, and the southern zone demonstrates an immediate (lag 0) response to JJA solar radiation (Fig. 3d). Overall, the relative importance of mean temperature and solar radiation for mangrove canopy greenness is further summarized in Fig. S3.

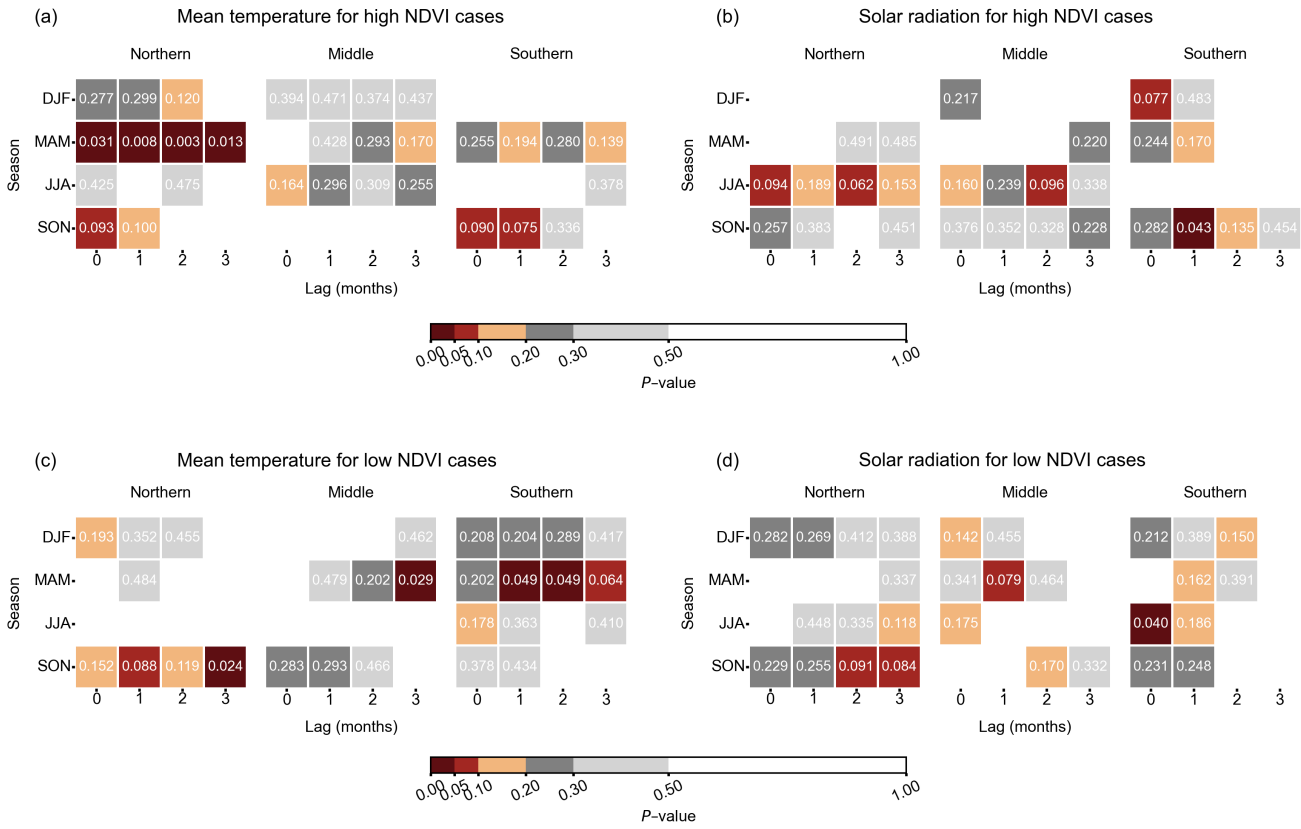


Figure 3. Time-lagged effect of mean temperature and solar radiation on mangrove canopy greenness in seasonal composites. Significance tests for associations of high NDVI cases with mean temperature (a) and solar radiation (b). Significance tests for associations of low NDVI cases with mean temperature (c) and solar radiation (d). Lags (τ) on the *x*-axis represent a three-month period that occurs τ months prior to a given season (*y*-axis). Statistical significance ($P < 0.10$) indicates significant lagged associations, with stronger evidence at $P < 0.05$. All *P*–values are rounded to three decimal places.

3.4 Climate-driven shifts in the thermal range of mangroves

Our findings highlight that temperature and solar radiation are significantly associated with regulating mangrove canopy greenness. To examine how future climate change may affect mangrove dynamics, we utilized multiple CMIP6 models to project future changes in mangrove dynamics across East Asia, where mangrove distribution is primarily constrained by minimum winter temperature thresholds (Osland et al., 2017). In Fujian Province, the critical biological threshold for mangrove survival is approximately 10 °C during winter (Wang et al., 2022). The spatial distribution of this critical isotherm is shown in Fig. 4a–b, comparing the CMIP6 baseline (2001–2022), constructed as described in 2.6, with projections for the late 21st century (2081–2100) under SSP3-7.0 and SSP1-2.6. Under both scenarios, the 10 °C winter isotherm shifts poleward relative to the historical period, with the shift being more pronounced under SSP3-7.0. This shift indicates a potential northward expansion of the temperature-defined range for mangrove establishment, potentially reaching northern Zhejiang Province in China, the southern coast of South Korea, and parts of Japan by the end of the 21st century.

However, projections indicate notable differences between the two scenarios. We compared projected temperature and solar radiation for the late 21st century (2081-2100) under SSP3-7.0 and SSP1-2.6 (Fig. 4a–b). Specifically, we focused on the DJF season, during which climatic factors can exert a significant influence on NDVI in the subsequent seasons in the northern zone (Fig. 2f; Fig. 3a). The results show that, although SSP3-7.0 projects winter (DJF) temperatures approximately 1.5°C higher than those under SSP1-2.6, this warming is accompanied by reduced solar radiation availability during critical growth periods. This pattern suggests that, while low-temperature constraints are unlikely to remain a major limitation under future warming, solar radiation may become a more important limiting factor. To further assess this possibility, we examined projected changes in the frequency of extreme low solar radiation events. Figures 4c–e illustrate trends in such events for both SSP3-7.0 and SSP1-2.6 scenarios during the seasons identified as important for NDVI in Fig. 3d. Under the SSP1-2.6 scenario, all three latitudinal zones exhibit declining trends in the frequency of these events. In contrast, the SSP3-7.0 scenario is characterized by increasing trends in low-radiation events across these zones.

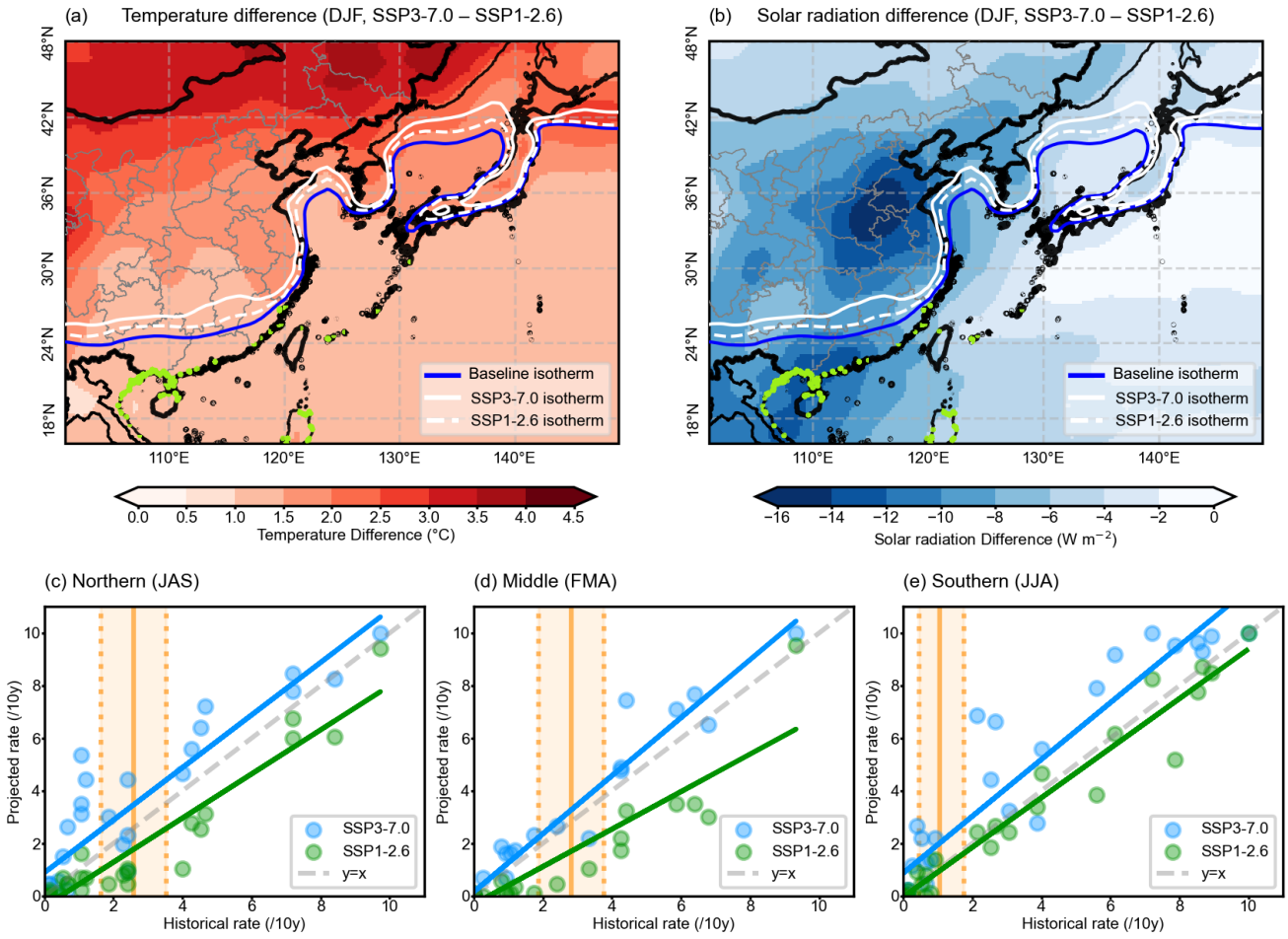


Figure 4. Mangrove dynamics driven by temperature and solar radiation in future scenarios. (a) Temperature difference in DJF for 2081–2100 (SSP3-7.0 – SSP1-2.6). (b) Solar radiation difference in DJF for 2081–2100 (SSP3-7.0 – SSP1-2.6). Green dots indicate the current distribution of mangroves in East Asia. Blue solid lines represent the baseline 10 °C DJF isotherm for 2001–2022, derived from CMIP6 historical simulations for 2001–2014 combined with SSP5-8.5 simulations for 2015–2022. White dashed, and white solid lines represent the corresponding future isotherms for 2081–2100 under SSP1-2.6 and SSP3-7.0, respectively. The baseline is common to both future scenarios. Panels (c–e) compare the rates of low solar radiation events simulated by 28 models for the northern (JAS; c), middle (FMA; d), and southern (JJA; e) zones. These windows correspond to significant associations with low NDVI in Fig. 3d at lags of 2, 1, and 0 months, respectively. The rate for the historical (1940–2014; *x*-axis) period is shown against those for SSP1-2.6 (2015–2100; *y*-axis, green) and SSP3-7.0 (2015–2100; *y*-axis, blue). The grey dashed line marks equal historical and future rates. The orange solid line represents the ERA5 event rate (1940–2024), and the orange dashed lines and shading mark its bootstrap interval from the 2.5th to 97.5th percentile.

We assessed future changes in temperature and solar radiation across the projected thermal range of mangroves in East Asia under the two climate scenarios. The potential impacts of high temperature and low solar radiation were evaluated using the thresholds derived from the northern zone in Fig 3a and 3d. CMIP6 models reproduced realistic ranges of mean temperature and solar radiation for the historical period, which largely encompass those of the observational dataset (Fig. 5, black lines

and blue shading), supporting their use for future projections. Our results indicate a substantial increase in the frequency with which key high-temperature thresholds are exceeded across the three regions (Fig. 5a–c). In comparison, projected changes in solar radiation show more limited shifts. Although SSP3-7.0 projects lower levels of solar radiation compared to SSP1-2.6 during the DJF season (Fig. 4b), solar radiation during the transitional season JAS does not show a significant decline relative to historical baselines, and the incidence of extreme low-radiation events remains limited (Fig. 5d–f). In contrast, the SSP1-2.6 shows a more pronounced increase in mean solar radiation, particularly during this transitional season (Fig. S4d–f), providing even more favourable conditions for photosynthesis and growth.

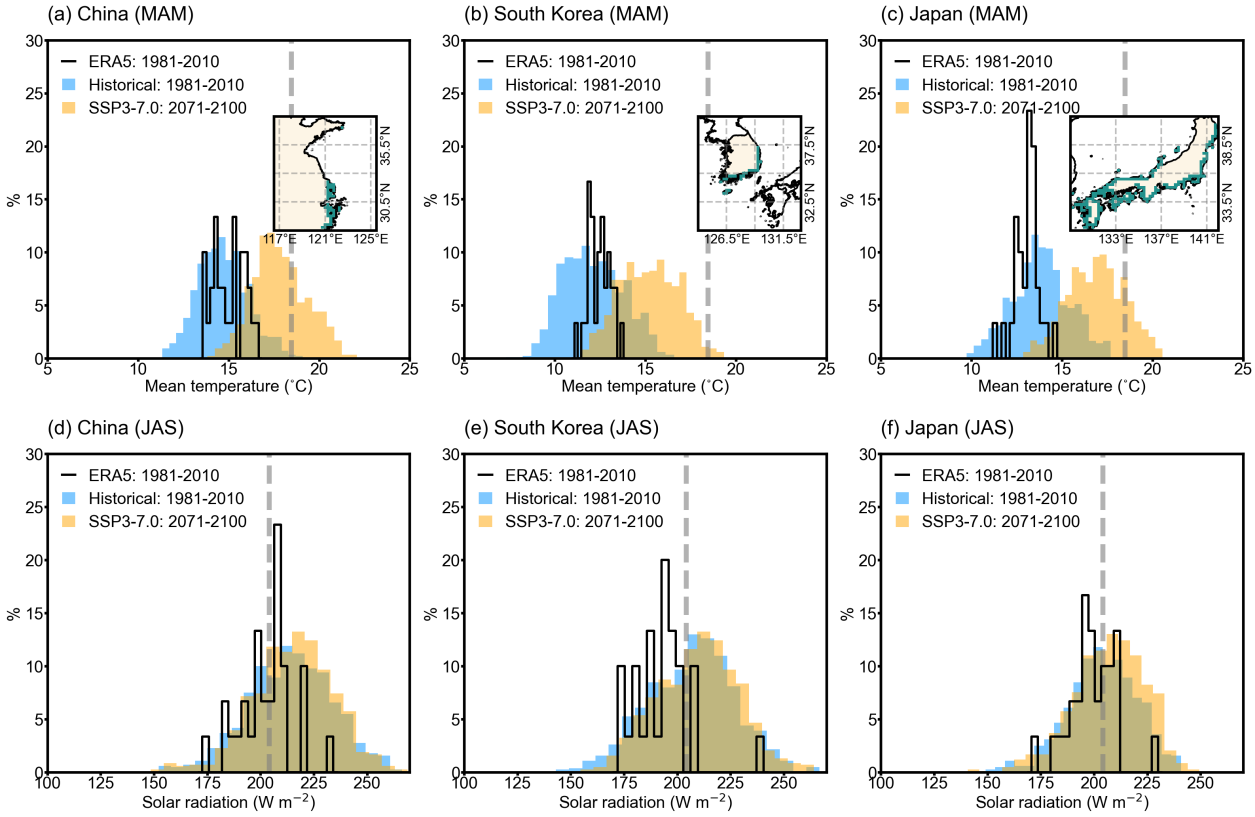


Figure 5. Changes in temperature and solar radiation within the future temperature-defined mangrove range. Histogram of mean temperature comparing ERA5 (1981–2010), CMIP historical (1981–2010) and SSP3-7.0 (2071–2100) for future potential mangrove habitats in China (a), South Korea (b) and Japan (c). Same but for solar radiation in China (d), South Korea (e) and Japan (f). The grey dashed lines represent the threshold criteria for high mean temperature (top row) and low solar radiation (bottom row), using the northern zone as the reference standard. The maps delineate potential mangrove habitats under SSP3-7.0 by integrating: (1) current non-mangrove shorelines, and (2) areas where winter (DJF) mean temperatures are projected to reach ≥ 10 °C in SSP3-7.0 (2071–2100). Other constraints on realized mangrove establishment, including intertidal habitat availability, shoreline hardening, sea-level rise, and dispersal, were not assessed.

4 Discussion

4.1 Spatial difference in mangrove NDVI patterns

Our results reveal pronounced latitudinal differences in the annual variation of mangrove NDVI across the three zones in Southeastern China. NDVI annual variability is largely aligned with the seasonal cycle of temperature in the northern and southern zones, whereas in the middle zone it is more strongly synchronized with variations in sunshine duration (Fig. 1b; Fig. S1). This pattern is likely attributable to the prevalence of cloud cover during the boreal spring associated with springtime mesoscale convective systems (Zhang et al., 2024a), which reduces incoming solar radiation and consequently limits photosynthetic activity and mangrove canopy development. Thus, solar radiation may act as a primary limiting factor for mangrove growth in the middle zone during this period. The annual mean and maximum NDVI distributions further highlight these latitudinal differences (Fig. 1c), with generally lower NDVI values in the northern zone and relatively high maximum values occurring more frequently in the middle and southern zones. These spatial and seasonal patterns are consistent with previous studies showing that mangrove vegetation responses vary across latitudinal gradients in association with climatic drivers such as temperature and solar radiation (Songsom et al., 2019). These differences may also partly reflect variation in species composition among the three zones, as different mangrove species can exhibit distinct seasonal NDVI responses, particularly during the winter–spring period (Li et al., 2019). For example, Hainan in the southern zone hosts the highest mangrove species diversity, whereas the middle zone is predominantly occupied by *Sonneratia apetala* and *Avicennia marina*, and the northern zone is mainly characterized by *K. obovata* (Zhao et al., 2024). The variation in dominant species composition may also contribute to the spatial differences across the three zones.

4.2 Solar radiation as a key regulator of mangrove greenness

Our results indicate that mangrove NDVI responds differently to climatic drivers, with linear regression analysis revealing that solar radiation exerts a broader influence on interannual variability in mangrove greenness than temperature (Fig. 2a–b). Although temperature is widely recognized as the principal limiting factor influencing the global distribution of mangroves, this effect is primarily reflected in the spatial distribution of species within our study region, shaped by species-specific thermal adaptation thresholds (Wu et al., 2018). Complementing these findings, extreme-case analysis further highlights the critical role of solar radiation in regulating mangrove growth (Fig. 2c–f). While solar radiation is fundamental for plant photosynthesis, its role in shaping mangrove phenology has often been underemphasized or considered secondary in previous studies examining climatic controls on mangrove ecosystems (Luo and Chui, 2020; Poungparn et al., 2020; Songsom et al., 2019). Nevertheless, some studies have highlighted the significant impact of solar radiation during specific phenological stages, such as seedling establishment and leaf senescence (Krauss et al., 2008; Sharma et al., 2012). Our findings extend this understanding by demonstrating a consistent positive influence of solar radiation on mangrove NDVI, underscoring its importance as a key environmental driver of mangrove greenness and potential productivity across latitudinal gradients.

The lagged-effect analysis also shows the importance of solar radiation (Fig. 3b, 3d). These patterns are particularly evident during seasonal transition periods, when mangroves undergo key phenological shifts associated with the onset, peak, and decline of the growing season. During such stages, carbon assimilation and utilization may become partially decoupled, with photosynthetic products being preferentially allocated to growth and reproduction during MAM (Trugman and Anderegg, 2024), and to canopy development prior to the peak growing season in JJA. In addition, increased solar radiation during late winter has been shown to advance the onset of the growing season in spring (Li et al., 2021), further highlighting the role of solar radiation in shaping mangrove phenology.

4.3 Lagged responses of mangrove NDVI to temperature

Temperature–NDVI relationships were less consistent across zones and months than the corresponding relationships with solar radiation (Fig. 2a–b). Although previous field studies documented cold damage (Chen et al., 2017; Zheng et al., 2016), the simultaneous DJF extreme-case analysis did not identify significant temperature associations in any of the three zones (Fig. S2a). This discrepancy may reflect the relative rarity of such chilling events in low-latitude regions or delayed responses of mangrove canopy greenness to extreme cold that are not captured by simultaneous relationships.

This interpretation was further supported by our lagged-effect analysis, which highlights the importance of phenological transition periods. For example, winter temperatures significantly influence subsequent spring mangrove canopy greenness across all three zones (Fig. 3a, 3c), indicating that MAM represents a sensitive period during which favourable climatic conditions accumulate to initiate the growing season (Wen et al., 2019). In the northern zone, mangrove species such as *K. obovata* are relatively cold-tolerant; however, higher winter temperatures remain beneficial, as low temperatures can induce persistent metabolic stress and impair the recovery of photosynthetic capacity, leading to subtle but lasting impacts on mangrove growth (Zheng et al., 2016). These results are supported by in-situ field surveys following the 2008 winter chilling event, which documented substantial mangrove defoliation in the middle and southern zones. Pronounced dieback was also observed in the southern zone, particularly among non-native species such as *S. apetala* (Chen et al., 2017). Moreover, our result indicates a significant influence of SON temperatures on mangrove canopy greenness (Fig. 3c). Higher autumn temperatures may extend the growing season and enhance photosynthetic activity (Peng et al., 2011; Songsom et al., 2019).

Overall, our results suggest that temperature variations within the normal thermal niche have limited influence on mangrove greenness, whereas extreme temperature events may exert more pronounced effects. This finding is consistent with previous studies suggesting that the proportion of hot days is a key factor influencing mangrove area (Luo and Chui, 2020).

4.4 Climate-driven trade-offs between future mangrove thermal range and growth

Our projections suggest a potential northward shift in the temperature-defined range for mangrove establishment, consistent with previous studies. Among mangrove species, *K. obovata* exhibits the highest cold tolerance and is a dominant species at the northern distribution limits of mangroves in both China and Japan (Analuddin et al., 2015; Chen et al., 2017; Khan and Kabir, 2017). It could therefore serve as a representative indicator species for potential range expansion. In southeastern

China, the natural northern limits of mangroves in Fujian Province have been projected to shift northward under future climate scenarios (Wang et al., 2022). Previous studies have further suggested that *K. obovata* could potentially establish along the southern coast of South Korea when the mean surface temperatures reach 10.4 °C in winter (Nam et al., 2024). It should be noted, however, that our projection represents a maximum potential northward extent of the temperature-defined range, rather than a prediction of the realized future distribution of mangroves. The actual establishment of mangroves depends on a more complex set of conditions and processes. These include local natural factors such as coastal substrate characteristics, topography, tidal and hydrological conditions, sediment dynamics, and propagule dispersal, all of which influence whether mangroves can successfully colonize and persist (Duke et al., 1998; Raw et al., 2019, 2023). In addition, anthropogenic pressures associated with coastal development and shoreline hardening may further constrain mangrove expansion (Leo et al., 2019).

Climate influences not only mangrove distribution but also their growth and productivity. Future projections suggest increasing temperature and a rise in low-solar-radiation events under SSP3-7.0 (Fig. 4c–e). This is particularly notable given previous studies reporting a general increase in surface solar radiation over southeastern China under the same scenario (Niu et al., 2023). However, such increasing trend is not uniform across all regions; in some localized areas, this signal is weak or even reversed. This highlights the importance of considering local variations in solar radiation in addition to large-scale trends. Furthermore, our results may indicate an increase in variability of solar radiation under SSP3-7.0 conditions. Such changes, beyond shifts in the mean state, may pose challenges for ecosystem resilience.

These patterns in solar radiation may be partly linked to aerosol forcing under SSP3-7.0 (Kim et al., 2024; Turnock et al., 2020). Previous studies have reported that under this scenario, global mean surface solar radiation declines by approximately 2.8 W m^{-2} during 2015–2100, primarily associated with global warming, with aerosol changes also modulating the magnitude of the decline (Song et al., 2025). While it has been suggested that the "diffuse fertilization effect"—an increase in diffuse radiation due to aerosols—can enhance vegetation productivity in some ecosystems (Mercado et al., 2009), the impacts of aerosols on mangrove photosynthetic efficiency remain uncertain. Although a rise in diffuse radiation may partially compensate for the reduction in direct solar radiation, evidence shows that reductions in aerosol concentrations, especially those achieved through air pollution control efforts, can positively influence ecosystem productivity. For example, it was reported that terrestrial net primary productivity in China recovered during 2014–2020 following the implementation of the Clean Air Action plan in 2013, largely attributable to aerosol reductions (Zhou et al., 2024). Nonetheless, some studies indicate that aerosol reductions may also induce unintended climatic consequences, such as regional warming and increased frequency of extreme weather events (Wang et al., 2023). These findings highlight the need for a nuanced approach to aerosol emission controls, including the prioritization of specific species such as black carbon, which is recognized as the second most potent anthropogenic climate forcing agent, exerting a positive radiative forcing of approximately +1.1 W m^{-2} (Bond et al., 2013).

Taken together, our results imply a potential ecological trade-off for mangrove ecosystems. On the one hand, rising temperatures may shift the thermal range of mangroves and enhance growth potential during sensitive growing periods. On

the other hand, the increasing occurrence of low-solar-radiation events may impose physiological or productivity constraints by limiting photosynthetic availability. Notably, the increasing risk of low-solar-radiation events appears to be concentrated within existing mangrove regions rather than in northern coastal areas newly meeting the selected temperature criterion. Consequently, under the SSP3-7.0 scenario, projected warming may expand the northward thermal range of mangroves, while sporadic low solar radiation events may still constrain productivity in some areas.

4.5 Challenges and implications for mangrove restoration in a changing climate

Mangroves are increasingly recognized as a nature-based climate solution due to their distinctive ecological functions and carbon sequestration capacity. In East Asia, mangrove restoration may therefore provide an additional opportunity to support climate change mitigation and national climate targets. Vegetated coastal wetlands, including mangroves and salt marshes, are increasingly incorporated into national blue-carbon and NDC frameworks, further increasing policy interest in their conservation and restoration (Arkema et al., 2023). However, translating this potential into on-the-ground afforestation efforts remains challenging.

One challenge highlighted by our results is the relatively high sensitivity of mangroves to climatic variability. Our comparison of lagged effects between mangroves and the nearby forests (Table S3) showed that mangroves are more strongly influenced by temperature during the MAM season. Previous research has also reported that global mangroves are experiencing higher interannual variability in productivity in comparison with forests (Zhang et al., 2024b). Together, these findings suggest that mangroves may be more sensitive to climatic variability, which increases the complexity and uncertainty associated with their restoration.

The practical challenges associated with mangrove restoration are also evident in the relatively low success rates reported from field-based restoration projects, ranging from 20–30% in China to 10–20% in the Philippines (Liao et al., 1996; Primavera and Esteban, 2008). These outcomes are often attributed to a combination of biotic and abiotic stresses, including low temperatures, high salinity, and unfavourable hydrological and tidal conditions. Restoration outcomes are also strongly influenced by species selection associated with both over- and under-adaptation. For example, the introduction of the non-native species *S. apetala*, although initially favoured for its rapid growth and high tolerance, has raised ecological concerns due to its potential to outcompete native species (Zhu et al., 2022). Moreover, it has shown vulnerability to extreme cold events, such as the 2008 chilling episode in Guangdong and Guangxi Provinces (Chen et al., 2017). In addition, species-specific differences in resilience to disturbances, such as typhoons, further complicate restoration efforts (Gao et al., 2025).

These findings highlight the importance of incorporating ecological suitability and climate resilience into mangrove restoration planning. Although our projections suggest that the thermal range of mangroves may shift poleward under future warming, successful restoration will depend on careful site selection that accounts for geographic, hydrological, and climatic variables (Lewis et al., 2019). Ultimately, effective mangrove afforestation in East Asia calls for interdisciplinary collaboration (Friess et al., 2022a), integrating ecologically-informed species selection, robust planting and management protocols, and long-term monitoring with adaptive governance frameworks.

4.6 Limitations and future perspectives

Despite these findings, several limitations should be acknowledged. First, because mangroves are typically distributed in narrow and fragmented coastal zones, the mismatch in spatial resolution between the NDVI and climate datasets may introduce uncertainties. In particular, the relatively coarse ERA5 data cannot fully resolve the fine-scale climatic heterogeneity experienced by individual mangrove stands. However, the climate–NDVI relationships examined in this study were evaluated at the regional scale. Therefore, the reported relationships should be interpreted as regional-scale instead of pixel-scale. Despite this limitation, ERA5 remains suitable for our regional-scale analysis because of its broad spatial coverage, temporal consistency, and long-term data availability. Second, the interaction between temperature and solar radiation was not examined in detail. Although the results from linear regression and bootstrapping suggested that their interaction was limited, this relationship warrants further investigation in future studies. Third, mangrove growth may also be influenced by additional climatic and environmental factors, such as precipitation, sea surface temperature, sea surface salinity, local topographic conditions, and tidal dynamics. In this study, however, we focused on temperature and solar radiation as fundamental climatic drivers that are applicable to both terrestrial forest ecosystems and intertidal mangrove systems. This does not imply that other factors are unimportant; instead, incorporating these additional environmental variables may provide a more comprehensive understanding of the drivers of mangrove vegetation dynamics and should be explored in future research.

In addition to these limitations, large-scale climate anomalies may exacerbate these uncertainties. For instance, a widespread mangrove dieback event occurred in the Gulf of Carpentaria between late 2015 and 2016, coinciding with a strong El Niño that brought extreme heat, low precipitation, and a temporary drop in sea level (Duke et al., 2017). The anticipated increase in frequency and intensity of extreme weather events and climate oscillations could introduce compounded stressors that challenge mangrove resilience in the future (Lovelock et al., 2022). Taken together, these findings suggest that while climate change presents opportunities for mangrove expansion and enhanced productivity, it simultaneously poses significant challenges. Balancing these dual outcomes will require integrated, multidisciplinary approaches that account for both anthropogenic and natural climate dynamics.

5 Conclusions

This study investigated the relationships between climate variability and mangrove NDVI along the South China Sea and assessed how future climate change may alter conditions relevant to mangrove growth across East Asia. Our results show that solar radiation, rather than temperature, exerts a more consistent control on mangrove NDVI variability across latitudinal zones, while extreme reductions in NDVI are associated with climatic anomalies exhibiting seasonal dependence. We further identified pronounced lagged effects of climatic drivers, with preceding winter temperatures influencing spring growth and solar radiation exerting seasonally dependent lagged controls, particularly during transitional periods of the growing season. Future projections suggest that continued warming may shift the thermal range of mangroves poleward in

East Asia by alleviating winter temperature constraints; however, an increased frequency of low solar radiation events under high-emission scenarios may partially offset these benefits by limiting mangrove growth. These findings highlight the importance of considering both solar radiation and lagged climatic effects when assessing the future dynamics and resilience of mangrove ecosystems under climate change. Incorporating these climatic controls may inform climate-resilient mangrove conservation and restoration in East Asia.

Data Availability

All datasets used in this study are publicly available. Mangrove distribution data were obtained from Global Mangrove Watch (https://zenodo.org/records/6894273). Land cover type data were obtained from MODIS Land Cover Type Yearly Global product (MCD12Q1) (https://www.earthdata.nasa.gov/data/catalog/lpcloud-mcd12q1-061). Remote sensing data for NDVI were obtained from MODIS Vegetation Indices (MOD13Q1) Version 6.1 (https://www.earthdata.nasa.gov/data/catalog/lpcloud-mod13q1-061). Climate data were obtained from European Centre for Medium-Range Weather Forecasts Reanalysis v5 (ERA5) (https://cds.climate.copernicus.eu/datasets/reanalysis-era5-single-levels-monthly-means?tab=overview). Data for total bright sunshine were obtained from Hong Kong Observatory (https://www.hko.gov.hk/sc/index.html). Earth System Models data were obtained from Coupled Model Intercomparison Project Phase 6 (CMIP6) (https://aims2.llnl.gov/search).

Competing interests

The authors declare that they have no conflict of interest.

Author contribution

RC conducted the data analysis and completed the manuscript. JK and HK contributed to the conceptualization and development of the research idea. JC, BL, SJ, and GS provided critical revisions and editorial support throughout the manuscript preparation.

Acknowledgments

This work was supported by Korea Environmental Industry & Technology Institute (KEITI) through 'Project for developing an observation-based GHG emissions geospatial information map', funded by Korea Ministry of Environment (MOE) (RS-2023-00232066). R. Chen and H.-J. Kim were supported by CityU Start-up Grant for New Faculty (Projects No. 9610581), Early Career Scheme (CityU 21300824) from the Hong Kong Research Grants Council (RGC) (Projects No. 9048306), and

the Center for Ocean Research in Hong Kong and Macau (CORE), which is a joint ocean research center for ocean research between Laoshan Laboratory and the Hong Kong University of Science and Technology.

References

Analuddin, K., Septiana, A., Sharma, S., and Hagihara, A.: Phenological Traits of Mangrove Kandelia obovata Grown in Manko Wetland, Okinawa Island, Japan, International Journal of Sustainable Tropical Agricultural Sciences, 2, 89–96, 2015.

Arkema, K. K., Delevaux, J. M. S., Silver, J. M., Winder, S. G., Schile-Beers, L. M., Bood, N., Crooks, S., Douthwaite, K., Durham, C., Hawthorne, P. L., Hickey, T., Mattis, C., Rosado, A., Ruckelshaus, M., von Unger, M., and Young, A.: Evidence-based target setting informs blue carbon strategies for nationally determined contributions, Nat Ecol Evol, 7, 1045–1059, https://doi.org/10.1038/s41559-023-02081-1, 2023.

Barbier, E. B., Hacker, S. D., Kennedy, C., Koch, E. W., Stier, A. C., and Silliman, B. R.: The value of estuarine and coastal ecosystem services, Ecological Monographs, 81, 169–193, https://doi.org/10.1890/10-1510.1, 2011.

Bond, T. C., Doherty, S. J., Fahey, D. W., Forster, P. M., Berntsen, T., DeAngelo, B. J., Flanner, M. G., Ghan, S., Kärcher, B., Koch, D., Kinne, S., Kondo, Y., Quinn, P. K., Sarofim, M. C., Schultz, M. G., Schulz, M., Venkataraman, C., Zhang, H., Zhang, S., Bellouin, N., Guttikunda, S. K., Hopke, P. K., Jacobson, M. Z., Kaiser, J. W., Klimont, Z., Lohmann, U., Schwarz, J. P., Shindell, D., Storelvmo, T., Warren, S. G., and Zender, C. S.: Bounding the role of black carbon in the climate system: A scientific assessment, Journal of Geophysical Research: Atmospheres, 118, 5380–5552, https://doi.org/10.1002/jgrd.50171, 2013.

Bunting, P., Rosenqvist, A., Hilarides, L., Lucas, R., Thomas, N., Tadono, T., Worthington, T., Spalding, M., Murray, N., and Rebelo, L.-M.: Global Mangrove Watch (1996 - 2020) Version 3.0 Dataset (3.0), https://doi.org/10.5281/zenodo.6894273, 2022.

Chen, L., Wang, W., Li, Q. Q., Zhang, Y., Yang, S., Osland, M. J., Huang, J., and Peng, C.: Mangrove species' responses to winter air temperature extremes in China, Ecosphere, 8, e01865, https://doi.org/10.1002/ecs2.1865, 2017.

Didan, K.: MODIS/Terra Vegetation Indices 16-Day L3 Global 250m SIN Grid V061, https://doi.org/10.5067/MODIS/MOD13Q1.061, 2021.

Ding, Y., Li, Z., and Peng, S.: Global analysis of time-lag and -accumulation effects of climate on vegetation growth, International Journal of Applied Earth Observation and Geoinformation, 92, 102179, https://doi.org/10.1016/j.jag.2020.102179, 2020.

Donato, D. C., Kauffman, J. B., Murdiyarso, D., Kurnianto, S., Stidham, M., and Kanninen, M.: Mangroves among the most carbon-rich forests in the tropics, Nature Geosci, 4, 293–297, https://doi.org/10.1038/ngeo1123, 2011.

Duke, N., Ball, M., and Ellison, J.: Factors influencing biodiversity and distributional gradients in mangroves, Global Ecology & Biogeography Letters, 7, 27–47, https://doi.org/10.1111/j.1466-8238.1998.00269.x, 1998.

Duke, N. C., Meynecke, J.-O., Dittmann, S., Ellison, A. M., Anger, K., Berger, U., Cannicci, S., Diele, K., Ewel, K. C., Field, C. D., Koedam, N., Lee, S. Y., Marchand, C., Nordhaus, I., and Dahdouh-Guebas, F.: A World Without Mangroves?, Science, 317, 41–42, https://doi.org/10.1126/science.317.5834.41b, 2007.

Duke, N. C., Kovacs, J. M., Griffiths, A. D., Preece, L., Hill, D. J. E., Oosterzee, P. van, Mackenzie, J., Morning, H. S., and Burrows, D.: Large-scale dieback of mangroves in Australia's Gulf of Carpentaria: a severe ecosystem response, coincidental with an unusually extreme weather event, Mar. Freshwater Res., 68, 1816–1829, https://doi.org/10.1071/MF16322, 2017.

Friess, D. A., Gatt, Y. M., Ahmad, R., Brown, B. M., Sidik, F., and Wodehouse, D.: Achieving ambitious mangrove restoration targets will need a transdisciplinary and evidence-informed approach, One Earth, 5, 456–460, https://doi.org/10.1016/j.oneear.2022.04.013, 2022a.

Friess, D. A., Adame, M. F., Adams, J. B., and Lovelock, C. E.: Mangrove forests under climate change in a 2°C world, WIREs Climate Change, 13, e792, https://doi.org/10.1002/wcc.792, 2022b.

Gao, X., Leung, F., and Wang, W.: Assessing typhoon impacts on mangroves and post-typhoon recovery patterns to inform projects using mangroves as nature-based solutions, Global Ecology and Conservation, 61, e03667, https://doi.org/10.1016/j.gecco.2025.e03667, 2025.

Goldberg, L., Lagomasino, D., Thomas, N., and Fatoyinbo, T.: Global declines in human-driven mangrove loss, Global Change Biology, 26, 5844–5855, https://doi.org/10.1111/gcb.15275, 2020.

Gultom, J. E. I., Hasibuan, H. S., and Patria, M. P.: Local Communities Participation in Mangrove Management for Tsunami Disaster Mitigation at Palu City Coastal, IOP Conf. Ser.: Earth Environ. Sci., 940, 012084, https://doi.org/10.1088/1755-1315/940/1/012084, 2021.

Hersbach, H., Bell, B., Berrisford, P., Biavati, G., Horányi, A., Muñoz Sabater, J., Nicolas, J., Peubey, C., Radu, R., Rozum, I., Schepers, D., Simmons, A., Soci, C., Dee, D., and Thépaut, J.-N.: ERA5 monthly averaged data on single levels from 1940 to present, Copernicus Climate Change Service (C3S) Climate Data Store (CDS), https://doi.org/10.24381/cds.f17050d7, 2023.

Jia, M., Wang, Z., Zhang, Y., Mao, D., and Wang, C.: Monitoring loss and recovery of mangrove forests during 42 years: The achievements of mangrove conservation in China, International Journal of Applied Earth Observation and Geoinformation, 73, 535–545, https://doi.org/10.1016/j.jag.2018.07.025, 2018.

Jia, M., Wang, Z., Mao, D., Ren, C., Song, K., Zhao, C., Wang, C., Xiao, X., and Wang, Y.: Mapping global distribution of mangrove forests at 10-m resolution, Science Bulletin, 68, 1306–1316, https://doi.org/10.1016/j.scib.2023.05.004, 2023.

Kainuma, M., Baba, S., Oshiro, N., Kezuka, M., and Chan, H. T.: Current Status of Mangroves Worldwide, Global Environmental Research, 17, 147–154, 2013.

Khan, M. N. and Kabir, M.: Ecology of Kandelia obovata (S., L.) Yong: A Fast-Growing Mangrove in Okinawa, Japan, 287–301, https://doi.org/10.1007/978-4-431-56481-2_18, 2017.

Kim, H.-J., Kim, J.-S., An, S.-I., Shin, J., Oh, J.-H., and Kug, J.-S.: Pervasive fire danger continued under a negative emission scenario, Nature Communications, 15, 10010, 2024.

Krauss, K. W., Lovelock, C. E., McKee, K. L., López-Hoffman, L., Ewe, S. M. L., and Sousa, W. P.: Environmental drivers in mangrove establishment and early development: A review, Aquatic Botany, 89, 105–127, https://doi.org/10.1016/j.aquabot.2007.12.014, 2008.

Kuwae, T., Yoshida, G., Hori, M., Watanabe, K., Tanaya, T., Okada, T., Umezawa, Y., and Sasaki, J.: Nationwide estimate of the annual uptake of atmospheric carbon dioxide by shallow coastal ecosystems in Japan, Journal of JSCE, 11, 2023.

Lee, B. and Baral, H.: Prospects of Adaptability and Establishment of Mangroves to Achieve Carbon Capture Expansion in Korean Coastal Areas, EGU-11394, https://doi.org/10.5194/egusphere-egu23-11394, 2023.

Lee C., Lee J., Kim C., Chu Y., and Lee B.: Prediction of Carbon Accumulation within Semi-Mangrove Ecosystems Using Remote Sensing and Artificial Intelligence Modeling in Jeju Island, South Korea, Ecology and Resilient Infrastructure, 10, 161–170, https://doi.org/10.17820/eri.2023.10.4.161, 2023.

Leo, K. L., Gillies, C. L., Fitzsimons, J. A., Hale, L. Z., and Beck, M. W.: Coastal habitat squeeze: A review of adaptation solutions for saltmarsh, mangrove and beach habitats, Ocean & Coastal Management, 175, 180–190, https://doi.org/10.1016/j.ocecoaman.2019.03.019, 2019.

Lewis, R. R., Brown, B. M., and Flynn, L. L.: Chapter 24 - Methods and Criteria for Successful Mangrove Forest Rehabilitation, in: Coastal Wetlands (Second Edition), edited by: Perillo, G. M. E., Wolanski, E., Cahoon, D. R., and Hopkinson, C. S., Elsevier, 863–887, https://doi.org/10.1016/B978-0-444-63893-9.00024-1, 2019.

Li, C., Wang, R., Cui, X., Wu, F., Yan, Y., Peng, Q., Qian, Z., and Xu, Y.: Responses of vegetation spring phenology to climatic factors in Xinjiang, China, Ecological Indicators, 124, 107286, https://doi.org/10.1016/j.ecolind.2020.107286, 2021.

Li, H., Jia, M., Zhang, R., Ren, Y., and Wen, X.: Incorporating the Plant Phenological Trajectory into Mangrove Species Mapping with Dense Time Series Sentinel-2 Imagery and the Google Earth Engine Platform, Remote Sensing, 11, 2479, https://doi.org/10.3390/rs11212479, 2019.

Liao, B., Zhen, D., and Zheng, S.: The present situation and prospect of mangrove afforestation in south China, Protection Forest Science and Technology, 4, 30–34, 1996.

Liu, H., Ren, H., Hui, D., Wang, W., Liao, B., and Cao, Q.: Carbon stocks and potential carbon storage in the mangrove forests of China, Journal of Environmental Management, 133, 86–93, https://doi.org/10.1016/j.jenvman.2013.11.037, 2014.

Lovelock, C. E., Barbier, E., and Duarte, C. M.: Tackling the mangrove restoration challenge, PLOS Biology, 20, e3001836, https://doi.org/10.1371/journal.pbio.3001836, 2022.

Luo, S. and Chui, T. F. M.: Annual variations in regional mangrove cover in southern China and potential macro- climatic and hydrological indicators, Ecological Indicators, 110, 105927, https://doi.org/10.1016/j.ecolind.2019.105927, 2020.

Macreadie, P. I., Costa, M. D. P., Atwood, T. B., Friess, D. A., Kelleway, J. J., Kennedy, H., Lovelock, C. E., Serrano, O., and Duarte, C. M.: Blue carbon as a natural climate solution, Nat Rev Earth Environ, 2, 826–839, https://doi.org/10.1038/s43017-021-00224-1, 2021.

Meinshausen, M., Nicholls, Z. R. J., Lewis, J., Gidden, M. J., Vogel, E., Freund, M., Beyerle, U., Gessner, C., Nauels, A., Bauer, N., Canadell, J. G., Daniel, J. S., John, A., Krummel, P. B., Luderer, G., Meinshausen, N., Montzka, S. A., Rayner, P. J., Reimann, S., Smith, S. J., van den Berg, M., Velders, G. J. M., Vollmer, M. K., and Wang, R. H. J.: The shared socio-economic pathway (SSP) greenhouse gas concentrations and their extensions to 2500, Geoscientific Model Development, 13, 3571–3605, https://doi.org/10.5194/gmd-13-3571-2020, 2020.

Mercado, L. M., Bellouin, N., Sitch, S., Boucher, O., Huntingford, C., Wild, M., and Cox, P. M.: Impact of changes in diffuse radiation on the global land carbon sink, Nature, 458, 1014–1017, https://doi.org/10.1038/nature07949, 2009.

Mooney, C. Z. and Duval, R. D.: Bootstrapping: A Nonparametric Approach to Statistical Inference, SAGE, 84 pp., 1993.

Nam, J., Yim, J., Park, J. Y., Kwon, B.-O., and Khim, J. S.: Determining the Likelihood of Mangrove Introduction to Korean Coastal Areas, Journal of Coastal Research, 116, https://doi.org/10.2112/JCR-SI116-066.1, 2024.

Nemani, R. R., Keeling, C. D., Hashimoto, H., Jolly, W. M., Piper, S. C., Tucker, C. J., Myneni, R. B., and Running, S. W.: Climate-Driven Increases in Global Terrestrial Net Primary Production from 1982 to 1999, Science, 300, 1560–1563, https://doi.org/10.1126/science.1082750, 2003.

Niu, J., Qin, W., Wang, L., Zhang, M., Wu, J., and Zhang, Y.: Climate change impact on photovoltaic power potential in China based on CMIP6 models, Science of The Total Environment, 858, 159776, https://doi.org/10.1016/j.scitotenv.2022.159776, 2023.

Osland, M. J., Feher, L. C., Griffith, K. T., Cavanaugh, K. C., Enwright, N. M., Day, R. H., Stagg, C. L., Krauss, K. W., Howard, R. J., Grace, J. B., and Rogers, K.: Climatic controls on the global distribution, abundance, and species richness of mangrove forests, Ecological Monographs, 87, 341–359, https://doi.org/10.1002/ecm.1248, 2017.

Pastor-Guzman, J., Dash, J., and Atkinson, P. M.: Remote sensing of mangrove forest phenology and its environmental drivers, Remote Sensing of Environment, 205, 71–84, https://doi.org/10.1016/j.rse.2017.11.009, 2018.

Peng, S., Chen, A., Xu, L., Cao, C., Fang, J., Myneni, R. B., Pinzon, J. E., Tucker, C. J., and Piao, S.: Recent change of vegetation growth trend in China, Environ. Res. Lett., 6, 044027, https://doi.org/10.1088/1748-9326/6/4/044027, 2011.

Poungparn, S., Komiyama, A., Umnouysin, S., Rodtassana, C., Sangtiean, T., Maknual, C., Pravinvongvuthi, T., Suchewaboripont, V., and Kato, S.: Ten-Year Estimation of Net Primary Productivity in a Mangrove Forest under a Tropical Monsoon Climate in Eastern Thailand: Significance of the Temperature Environment in the Dry Season, Forests, 11, 987, https://doi.org/10.3390/f11090987, 2020.

Primavera, J. H. and Esteban, J. M. A.: A review of mangrove rehabilitation in the Philippines: successes, failures and future prospects, Wetlands Ecol Manage, 16, 345–358, https://doi.org/10.1007/s11273-008-9101-y, 2008.

Raw, J. L., Godbold, J. A., van Niekerk, L., and Adams, J. B.: Drivers of mangrove distribution at the high-energy, wave-dominated, southern African range limit, Estuarine, Coastal and Shelf Science, 226, 106296, https://doi.org/10.1016/j.ecss.2019.106296, 2019.

Raw, J. L., Van der Stocken, T., Carroll, D., Harris, L. R., Rajkaran, A., Van Niekerk, L., and Adams, J. B.: Dispersal and coastal geomorphology limit potential for mangrove range expansion under climate change, Journal of Ecology, 111, 139–155, https://doi.org/10.1111/1365-2745.14020, 2023.

Reef, R. and Lovelock, C. E.: Regulation of water balance in mangroves, Annals of Botany, 115, 385–395, https://doi.org/10.1093/aob/mcu174, 2015.

Sasmito, S. D., Basyuni, M., Kridalaksana, A., Saragi-Sasmito, M. F., Lovelock, C. E., and Murdiyarso, D.: Challenges and opportunities for achieving Sustainable Development Goals through restoration of Indonesia's mangroves, Nat Ecol Evol, 7, 62–70, https://doi.org/10.1038/s41559-022-01926-5, 2023.

Sharma, S., Kamruzzaman, Md., Rafiqul Hoque, A. T. M., and Hagihara, A.: Leaf phenological traits and leaf longevity of three mangrove species (Rhizophoraceae) on Okinawa Island, Japan, J Oceanogr, 68, 831–840, https://doi.org/10.1007/s10872-012-0133-9, 2012.

Song, F., Mao, Y., Liu, S., Wu, L., Dong, L., Su, H., Wang, Y., Chtirkova, B., Wu, P., and Wild, M.: A long-term decline in downward surface solar radiation, National Science Review, 12, nwaf007, https://doi.org/10.1093/nsr/nwaf007, 2025.

Songsom, V., Koedsin, W., Ritchie, R. J., and Huete, A.: Mangrove Phenology and Environmental Drivers Derived from Remote Sensing in Southern Thailand, Remote Sensing, 11, 955, https://doi.org/10.3390/rs11080955, 2019.

Sulla-Menashe, D. and Friedl, M. A.: User Guide to Collection 6 MODIS Land Cover (MCD12Q1 and MCD12C1) Product, 2018.

Tran, T. V., Reef, R., and Zhu, X.: A Review of Spectral Indices for Mangrove Remote Sensing, Remote Sensing, 14, 4868, https://doi.org/10.3390/rs14194868, 2022.

Trugman, A. T. and Anderegg, L. D. L.: Source vs sink limitations on tree growth: from physiological mechanisms to evolutionary constraints and terrestrial carbon cycle implications, New Phytologist, https://doi.org/10.1111/nph.20294, 2024.

Turnock, S. T., Allen, R. J., Andrews, M., Bauer, S. E., Deushi, M., Emmons, L., Good, P., Horowitz, L., John, J. G., Michou, M., Nabat, P., Naik, V., Neubauer, D., O'Connor, F. M., Olivié, D., Oshima, N., Schulz, M., Sellar, A., Shim, S., Takemura, T., Tilmes, S., Tsigaridis, K., Wu, T., and Zhang, J.: Historical and future changes in air pollutants from CMIP6 models, Atmospheric Chemistry and Physics, 20, 14547–14579, https://doi.org/10.5194/acp-20-14547-2020, 2020.

Wang, P., Yang, Y., Xue, D., Ren, L., Tang, J., Leung, L. R., and Liao, H.: Aerosols overtake greenhouse gases causing a warmer climate and more weather extremes toward carbon neutrality, Nat Commun, 14, 7257, https://doi.org/10.1038/s41467-023-42891-2, 2023.

Wang, Y., Dong, P., Hu, W., Chen, G., Zhang, D., Chen, B., and Lei, G.: Modeling the Climate Suitability of Northernmost Mangroves in China under Climate Change Scenarios, Forests, 13, 64, https://doi.org/10.3390/f13010064, 2022.

Wen, Y., Liu, X., Xin, Q., Wu, J., Xu, X., Pei, F., Li, X., Du, G., Cai, Y., Lin, K., Yang, J., and Wang, Y.: Cumulative Effects of Climatic Factors on Terrestrial Vegetation Growth, Journal of Geophysical Research: Biogeosciences, 124, 789–806, https://doi.org/10.1029/2018JG004751, 2019.

Winkler, A. J., Myneni, R. B., and Brovkin, V.: Investigating the applicability of emergent constraints, Earth System Dynamics, 10, 501–523, https://doi.org/10.5194/esd-10-501-2019, 2019.

Wu, Y., Ricklefs, R. E., Huang, Z., Zan, Q., and Yu, S.: Winter temperature structures mangrove species distributions and assemblage composition in China, Global Ecology and Biogeography, 27, 1492–1506, https://doi.org/10.1111/geb.12826, 2018.

Xu, X., Fu, D., Su, F., Lyne, V., Yu, H., Tang, J., Hong, X., and Wang, J.: Global distribution and decline of mangrove coastal protection extends far beyond area loss, Nat Commun, 15, 10267, https://doi.org/10.1038/s41467-024-54349-0, 2024.

Zhang, L., Fu, T.-M., Hu, Z., Liu, H., Meng, Z., Ma, L., Dai, J., and Zhang, F.: Springtime mesoscale convective systems over South China: a historic radar image-based analysis of climatological features, interannual variability, and potential connections with surface aerosol, Environ. Res. Lett., 19, 024026, https://doi.org/10.1088/1748-9326/ad2024, 2024a.

Zhang, Z., Luo, X., Friess, D. A., Wang, S., Li, Y., and Li, Y.: Stronger increases but greater variability in global mangrove productivity compared to that of adjacent terrestrial forests, Nat Ecol Evol, 1–12, https://doi.org/10.1038/s41559-023-02264-w, 2024b.

Zhao, C., Jia, M., Zhang, R., Wang, Z., Ren, C., Mao, D., and Wang, Y.: Mangrove species mapping in coastal China using synthesized Sentinel-2 high-separability images, Remote Sensing of Environment, 307, 114151, https://doi.org/10.1016/j.rse.2024.114151, 2024.

Zheng, C., Tang, J., Chen, J., Liu, W., Qiu, J., Peng, X., and Ye, Y.: Mechanisms on inhibition of photosynthesis in Kandelia obovata due to extreme cold events under climate change, Ecological Processes, 5, 20, https://doi.org/10.1186/s13717-016-0064-2, 2016.

Zhou, H., Yue, X., Dai, H., Geng, G., Yuan, W., Chen, J., Shen, G., Zhang, T., Zhu, J., and Liao, H.: Recovery of ecosystem productivity in China due to the Clean Air Action plan, Nat. Geosci., 17, 1233–1239, https://doi.org/10.1038/s41561-024-01586-z, 2024.

Zhu, D., Hui, D., Huang, Z., Qiao, X., Tong, S., Wang, M., Yang, Q., and Yu, S.: Comparative impact of light and neighbor effect on the growth of introduced species Sonneratia apetala and native mangrove species in China: implications for restoration, Restoration Ecology, 30, e13522, https://doi.org/10.1111/rec.13522, 2022.

Zuzulova, V. and Vido, J.: Normalized difference vegetation index as a tool for the evaluation of agricultural drought in Slovakia, Ecocycles, 4, 83–87, https://doi.org/10.19040/ecocycles.v4i1.124, 2018.